Helical magnetorotational instability in magnetized Taylor-Couette flow

Wei Liu,[1,*] Jeremy Goodman,[2] Isom Herron,[3] and Hantao Ji[1]
[1]*Center for Magnetic Self-Organization in Laboratory and Astrophysical Plasma, Princeton Plasma Physics Laboratory, Princeton University, P.O. Box 451, Princeton, New Jersey 08543, USA*
[2]*Princeton University Observatory, Princeton, New Jersey 08544, USA*
[3]*Department of Mathematical Sciences, Rensselaer Polytechnic Institute, Troy, New York 12180, USA*
(Received 6 June 2006; published 7 November 2006)

Hollerbach and Rüdiger have reported a new type of magnetorotational instability (MRI) in magnetized Taylor-Couette flow in the presence of combined axial and azimuthal magnetic fields. The salient advantage of this "helical" MRI (HMRI) is that marginal instability occurs at arbitrarily low magnetic Reynolds and Lundquist numbers, suggesting that HMRI might be easier to realize than standard MRI (axial field only), and that it might be relevant to cooler astrophysical disks, especially those around protostars, which may be quite resistive. We confirm previous results for marginal stability and calculate HMRI growth rates. We show that in the resistive limit, HMRI is a weakly destabilized inertial oscillation propagating in a unique direction along the axis. But we report other features of HMRI that make it less attractive for experiments and for resistive astrophysical disks. Large axial currents are required. More fundamentally, instability of highly resistive flow is peculiar to infinitely long or periodic cylinders: finite cylinders with insulating endcaps are shown to be stable in this limit, at least if viscosity is neglected. Also, Keplerian rotation profiles are stable in the resistive limit regardless of axial boundary conditions. Nevertheless, the addition of a toroidal field lowers thresholds for instability even in finite cylinders.

DOI: 10.1103/PhysRevE.74.056302 PACS number(s): 47.20.−k, 47.65.−d, 52.30.Cv, 52.72.+v

I. INTRODUCTION

The magnetorotational instability (MRI) is probably the main source of turbulence and accretion in sufficiently ionized astrophysical disks [1]. MRI was first discovered theoretically [2–4], then later supported numerically [5–7], but has never been directly observed in astronomy. No unambiguous laboratory study of MRI has been completed, notwithstanding the claims of Sisan *et al.* [8], whose experiment proceeded from a background state that was not in MHD equilibrium, nor Ref. [9] (see Sec. III). We and others therefore have proposed experimental demonstrations of MRI [10–12]. The experimental geometry planned by most groups is a magnetized Taylor-Couette flow: an incompressible liquid metal confined between concentric rotating cylinders, with an imposed background magnetic field sustained by currents external to the fluid.

The challenge for experimentation, however, is that liquid-metal flows are very far from ideal on laboratory scales. While the fluid Reynolds number $\mathrm{Re}\equiv\Omega_1 r_1(r_2-r_1)/\nu$ can be large, the corresponding *magnetic* Reynolds number $\mathrm{Re_m}\equiv\Omega_1 r_1(r_2-r_1)/\eta$ is modest or small because the magnetic Prandtl number $\mathrm{Pr_m}\equiv\nu/\eta\sim 10^{-5}-10^{-6}$ in liquid metals; here $\nu\lesssim 10^{-2}\ \mathrm{cm^2\ s^{-1}}$ is the kinematic viscosity and η is the magnetic diffusivity. Standard MRI modes will not grow unless both the rotation period and the Alfvén crossing time are shorter than the time scale for magnetic diffusion. This requires both $\mathrm{Re_m}\gtrsim 1$ and $S\gtrsim 1$, where $S\equiv V_A(r_2-r_1)/\eta$ is the Lundquist number, and $V_A=B/\sqrt{\mu_0\rho}$ is the Alfvén speed. Therefore $\mathrm{Re}\gtrsim 10^6$ and fields of several kilogauss must typically be achieved.

Recently, Hollerbach and collaborators have discovered that MRI-like modes may grow at much reduced $\mathrm{Re_m}$ and S in the presence of a helical background field, a current-free combination of axial and toroidal field [13,14].

$$\boldsymbol{B}^{(0)}=B_z^{(0)}\left(\boldsymbol{e}_z+\beta\frac{r_1}{r}\boldsymbol{e}_\theta\right) \tag{1}$$

in cylindrical coordinates (r,θ,z), where $B_z^{(0)}$ and β are constants. [When it will not cause ambiguity, we will omit the superscript (0) from $\boldsymbol{B}$ and B_z hereafter.] Henceforth, "standard MRI" (SMRI) will refer to cases where the $\beta=0$, and "helical MRI" (HMRI) to modes that require $\beta\neq 0$. In centrifugally stable flows—meaning that $d(r^2\Omega)^2/dr>0$, where $\Omega=V_\theta^{(0)}/r$ is the background angular velocity—SMRI exists only when $\mathrm{Re_m}$ and S exceed thresholds of order unity [10,11]. Remarkably, however, HMRI may persist in such flows even as both parameters tend to zero, though not independently: more precisely, the thresholds are $\ll 1$ and would vanish if the fluid were inviscid ($\nu=0$). In a fixed geometry and flow profile, the resistive limit may be approached theoretically by increasing η with all other parameters held constant. The growth rate of inviscid HMRI is then $\propto\eta^{-1}$ so that the hydrodynamic case is approached continuously. The special case of toroidal-only magnetic field ($\beta=\infty$) is stable [15].

Our own interest in HMRI stems as much from astrophysical as from experimental considerations. Accretion disks composed of substantially ionized plasma tend to be in the ideal MHD limit: $\mathrm{Re_m}\gg 1$ and $S\gg 1$; also $\mathrm{Pr_m}\gg 1$. The disks around protostars, in which planets form, are cool and very weakly ionized, however. If their ionization fractions followed thermal equilibrium, such disks would be far too resistive for SMRI, but the actual resistivity is uncertain be-

*Email address: wliu@pppl.gov

cause it involves stellar x rays and other nonthermal sources of ionization, as well as recombination rates that are sensitive to the unknown abundance of small dust grains [16,17]. The fluid Reynolds number of protostellar disks is in any case very large, $\mathrm{Re}\sim 10^{12}$, and therefore $\mathrm{Pr_m}$ is surely even smaller than in liquid metals.

A feature of the background state for HMRI is that there is a uniform axial flux of angular momentum carried by the field, $rT_{\varphi z}^{(\mathrm{mag})}=-rB_\theta B_z/\mu_0$ and an associated axial Poynting flux Ω times this. In an infinite or periodic cylinder, the question of the sources and sinks of these axial fluxes need not arise, but in an experimental device, a torque is exerted by the axial field on the radial sections of the coil that complete the circuit containing the axial current. Related to this perhaps, the dispersion relation for linear modes is sensitive to the sign of the axial wave number (k_z), and the instabilities of axially infinite or periodic cylinders are traveling rather than standing waves, as noted by Knobloch [18,19]. This begs the question what should happen to the modes in finite cylinders, a question that has motivated much of our analysis.

Even the analysis for periodic cylinders implies two practical difficulties for an HMRI experiment. First, as will be seen, the typical growth rates tend to be smaller than those of SMRI except in regimes where SMRI would also be unstable. This is largely a consequence of looking for HMRI at lower rotation rates; when normalized to the rotation rates of the cylinders, the growth rates of HMRI and resistive SMRI can be comparable. In practice, the ease with which growth can be discerned probably depends less upon the ratio γ/Ω of growth rate to rotation rate than upon γt_E, where t_E is the Ekman circulation time. Since $\Omega t_E\propto \mathrm{Re}^{-1/2}$, Ekman circulation may be more problematic at the lower Reynolds numbers where HMRI is unstable but SMRI is not. A second difficulty is the axial current needed for the required toroidal fields tends to be quite large: $I[\mathrm{kA}]=5B_\theta r[\mathrm{kG\ cm}]$. This is partly offset by the low Re and $\mathrm{Re_m}$ needed for HMRI, which permits a radially compact apparatus. Despite these difficulties, experimental verification of HMRI has already been claimed in a recent paper [9].

In Sec. II we analyze the linear stability of HMRI using complementary approximations, some for infinite/periodic cylinders and others for finite ones. The results are compared with one another and with fully nonlinear axisymmetric simulations. Our conclusions are summarized in Sec. III.

II. LINEAR THEORY

All magnetic fields are expressed as Alfvén speeds, in other words, units such that $\mu_0=1/\rho$ are used. Uppercase letters are used for the background magnetic field (1) and velocity $\boldsymbol{V}=r\Omega(r)\boldsymbol{e}_\theta$, and lowercase $(\boldsymbol{b},\boldsymbol{v})$ for perturbations. Frequently occurring derivatives are abbreviated by $\partial_r^\dagger\equiv\partial_r+r^{-1}$, $D\equiv\partial_r\partial_r^\dagger+\partial_z^2$. Incompressibility allows the use of stream functions for the poloidal components: $v_r=\partial_z\phi$, $v_z=-\partial_r^\dagger\phi$, $b_r=\partial_z\psi$, $b_z=-\partial_r^\dagger\psi$; note that these definitions differ by factors of r from the usual ones. The linearized inviscid MHD equations then become, since B_z and rB_θ are constant,

$$(\underline{\partial_t}-\eta D)\psi=B_z\partial_z\phi, \tag{2}$$

$$(\underline{\partial_t}-\eta D)b_\theta=\partial_z\left(\frac{2B_\theta}{r}\phi+B_z v_\theta+\underline{r\Omega'\psi}\right), \tag{3}$$

$$\partial_t D\phi-2\Omega\partial_z v_\theta=B_z\partial_z D\psi-\frac{2B_\theta}{r}\partial_z b_\theta, \tag{4}$$

$$\partial_t v_\theta+r^{-1}(r^2\Omega)'\partial_z\phi=B_z\partial_z b_\theta. \tag{5}$$

The underlined terms above are negligible in the resistive limit, where $\boldsymbol{b}$ scales $\propto\eta^{-1}$ compared to $\boldsymbol{v}$. Neglecting these terms has been shown to suppress SMRI [11,20], but not HMRI as will be seen.

Taking another time derivative of Eq. (4) and eliminating $\partial_t v_\theta$ *via* Eq. (5) yields

$$(\partial_t^2 D+\kappa^2\partial_z^2)\phi=B_z\partial_z\partial_t D\psi+2\left(\Omega B_z\partial_z^2-\frac{B_\theta}{r}\partial_z\partial_t\right)b_\theta, \tag{6}$$

in which $\kappa^2\equiv r^{-3}d(r^2\Omega)^2/dr^2$ is the square of the epicyclic frequency. As $\eta\to\infty$, Eq. (6) reduces to

$$(\partial_r\partial_r^\dagger+\partial_z^2)\partial_t^2\phi+\kappa^2(r)\partial_z^2\phi=0. \tag{7}$$

A. WKB for infinite or periodic cylinders

If we take the gap to be narrow, $d\equiv r_2-r_1\ll r$, then it is reasonable to treat r, B_z, Ω, $r\Omega'=2\,\mathrm{Ro}\,\Omega$, and $r^{-1}(r^2\Omega)'=2(1+\mathrm{Ro})\Omega=\kappa^2/2\Omega$ as constants, and to look for perturbations $\propto\exp(ik_r r+ik_z z-i\omega t)$. The Rossby number $\mathrm{Ro}\equiv\frac{1}{2}d\ln\Omega/d\ln r$ has been introduced. In this case one expects to have WKB solutions with D replaced by $-(k_r^2+k_z^2)\equiv K^2$, where the total wave number $K=O(d^{-1})$.

When applied to Eq. (7) (i.e., for $\eta\to\infty$) these prescriptions yield the dispersion relation for hydrodynamic inertial oscillations (hereafter IO),

$$\omega_{\mathrm{IO}}^2=\kappa^2\frac{k_z^2}{k_r^2+k_z^2}\quad\text{where}\quad\kappa^2=\frac{1}{r^3}\frac{d}{dr}(r^2\Omega)^2=4(1+\mathrm{Ro})\Omega^2. \tag{8}$$

IO exist only in the Rayleigh-stable regime $\kappa^2>0$, $\mathrm{Ro}>-1$, and their frequencies lie between 0 and κ.

HMRI occurs at finite η when $B_\theta/r\equiv\omega_\theta$ is comparable to $k_z B_z\equiv\omega_z$. Define $\omega_\eta\equiv\eta K^2$ and $\mu\equiv k_z/|K|\in[-1,1]$. The dispersion relation corresponding to the system (2)–(5) is then

$$\begin{aligned}0=&s^4+2\omega_\eta s^3+[\omega_\eta^2+4\mu^2\omega_\theta^2+2\omega_z^2+\mu^2\kappa^2]s^2+2[2\omega_\eta\mu^2\omega_\theta^2\\&+\omega_\eta\omega_z^2+\omega_\eta\mu^2\kappa^2-4i\mu^2\omega_\theta\omega_z\Omega]s+[\omega_\eta^2\mu^2\kappa^2\\&-4i\omega_\eta\omega_\theta\omega_z\mu^2\Omega(2+\mathrm{Ro})+\omega_z^4+4\mu^2\omega_z^2\Omega^2\,\mathrm{Ro}],\end{aligned} \tag{9}$$

where the complex growth rate $s\equiv-i\omega$ has been used so that the coefficients are all real except for those linear in ω_θ. It is instructive to consider the limit in which ω_η is much larger than all of the other frequencies, including ω:

$$\begin{aligned}s^2+\omega_{\mathrm{IO}}^2+2\omega_\eta^{-1}[&s^3+(2\mu^2\omega_\theta^2+\omega_z^2+\omega_{\mathrm{IO}}^2)s\\&-2i\omega_\theta\omega_z\mu^2\Omega(2+\mathrm{Ro})]\approx O(\omega_\eta^{-2}).\end{aligned} \tag{10}$$

The replacement $\mu^2\kappa^2\to\omega_{\mathrm{IO}}^2$ emphasizes that $\omega\approx\pm\omega_{\mathrm{IO}}$ in this limit. The roots are

$$\omega \approx \mp \omega_{\mathrm{IO}} + i\omega_\eta^{-1}[\pm 2\omega_\theta\omega_z\omega_{\mathrm{IO}}^{-1}\mu^2\Omega(2+\mathrm{Ro}) - (2\mu^2\omega_\theta^2 + \omega_z^2)] + O(\omega_\eta^{-2}), \quad (11)$$

the bivalent signs being correlated. The other two roots of Eq. (9) represent rapidly decaying magnetic perturbations, $s \approx -\omega_\eta$.

We conclude that *in highly resistive flow, HMRI reduces to a weakly destabilized inertial oscillation*. In the present inviscid approximation, instability persists to arbitrarily large resistivity, though with reduced growth rate. Furthermore, we note from Eq. (11) that instability [i.e., $\mathrm{Im}(\omega) > 0$] occurs only if the bivalent signs are chosen so that $\Omega B_\theta B_z k_z / \mathrm{Re}(\omega) < 0$, which implies that *the unstable mode propagates axially with the same sense as the background Poynting flux*. [From Eq. (8), the group velocity $\partial \mathrm{Re}(\omega)/\partial k_z$ and phase velocity $\mathrm{Re}(\omega)/k_z$ have the same sign.] Although we have derived this propagation rule in the resistive limit, numerical evidence indicates that it is true of the full dispersion relation (9), as demonstrated by Figure. 1.

Instability requires the square brackets in Eq. (11) to be positive, whence

$$2(\mu\omega_\theta)^2 \pm \frac{2+\mathrm{Ro}}{\sqrt{1+\mathrm{Ro}}}\omega_z(\mu\omega_\theta) + \omega_z^2 < 0.$$

The inequality is possible if and only if the discriminant of the left-hand side, regarded as a quadratic equation in $\mu\omega_\theta$, is positive:

$$\frac{(2+\mathrm{Ro})^2}{1+\mathrm{Ro}}\omega_z^2 - 8\omega_z^2 > 0,$$

which translates to

$$\mathrm{Ro} < 2(1-\sqrt{2}) \approx -0.8284 \ \underline{\mathrm{or}} \ \mathrm{Ro} > 2(1+\sqrt{2}) \approx 4.8284. \quad (12)$$

Thus, within WKB, at least for highly resistive but inviscid flow ($\mathrm{Re}_m, S \to 0^+$, $\mathrm{Re} \to \infty$), the Keplerian value $\mathrm{Ro} = -3/4$ is excluded, as of course is uniform rotation ($\mathrm{Ro} = 0$)). We say "of course" because, the background being current free, the only source of free energy is the shear.

B. Numerical results for wide gaps in periodic cylinders

We have adapted a code developed by [11] to allow for a helical field. Vertical periodicity is assumed, but the radial equations are solved directly by finite differences with perfectly conducting boundary conditions. The underlined terms in Eqs. (2)–(5) are retained, and viscous terms are added although their influence is small at Reynolds numbers of interest. The code reproduces published results for marginal stability [14,13]. Table I compares the predictions of the WKB dispersion relation (9) with those of this code (labeled "Global"). The agreement is reasonably good, considering the crudeness of the WKB approximation. No unstable modes are found for the parameters of Fig. 1 at $\mathrm{Ro}(r_1) \geqslant -0.80$: the Keplerian value $\mathrm{Ro} = -0.75$ is stable.

Astrophysical disks correspond to very wide gaps, $r_2 - r_1 \gg h$, as well as Keplerian rotation. Given $(\mathrm{Re}_m, S) = (0.1, 0.03)$ and $r_2/r_1 = 2.0$, 2.83, and 5.0, the maximum unstable Rossby numbers at the inner cylinder are found to be $\mathrm{Ro}(r_1) = -0.88$, -0.92, and -0.95, respectively, from our radially global linear code. We conjecture that Keplerian flows—more precisely, flows in which $0 \geqslant \mathrm{Ro} \geqslant -3/4$ at all radii—are stable for all gap widths. It would be interesting to prove this.

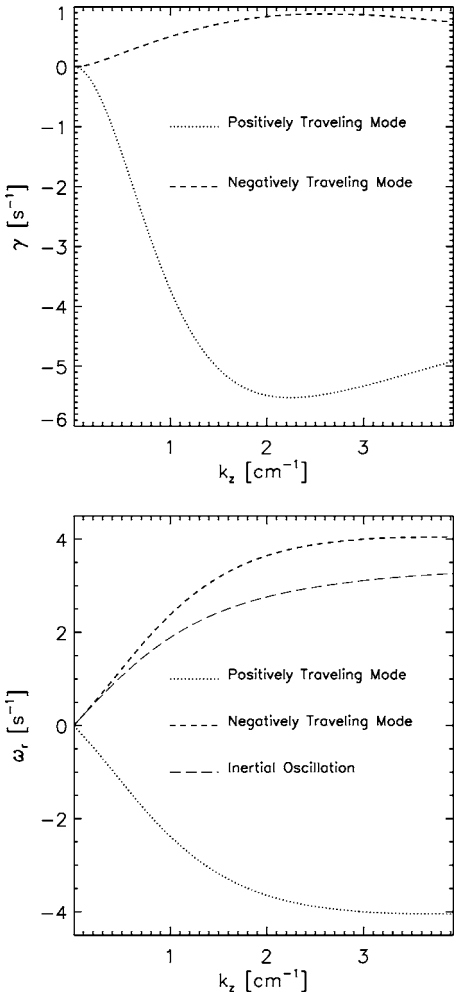

FIG. 1. Selected roots of full dispersion relation (9) for $\eta = 2000\ \mathrm{cm^2\ s^{-1}}$ [gallium], $r_1 = 9$ cm, $r_2 = 11$ cm, vertical periodicity $2h = 16$ cm, $\Omega_1 = 100$ rpm, $\Omega_2 = 68.1$ rpm, $B_z = 500$ G, $B_\theta = 10$ kG at $r = (r_1 + r_2)/2$. The two rapidly damped modes are omitted. (a) Growth rate $\gamma = \mathrm{Im}\omega$ vs. wave number k_z (b) Real frequency $\omega_r = \mathrm{Re}\omega$ vs. wave Number k_z

We have also estimated a few growth rates with our nonlinear, compressible nonideal MHD code [21], which is a modified version of the astrophysical code ZEUS2D [22]. In this case, we use the wide-gap geometry of the Princeton MRI experiment [10,11], except that the computation uses periodic vertical boundaries: $r_1 = 7.1$ cm, $r_2 = 20.3$ cm, $h = 27.9$ cm, $\Omega_1 = 400$ rpm, $\Omega_2 = 53.3$ rpm, $B_z = 500$ G, and $B_\theta(r_1) = 1$ kG; the material properties are again based on gallium: $\eta \approx 2000\ \mathrm{cm^2\ s^{-1}}$, $\nu \approx 3 \times 10^{-3}\ \mathrm{cm^2\ s^{-1}}$. The growth rate and real frequency from the ZEUS2D simulations are, respectively, 1.06 and $3.93\ \mathrm{s^{-1}}$, compared to 1.05 and $3.89\ \mathrm{s^{-1}}$ from the linear code. WKB yields (γ, ω_r)

TABLE I. Comparison between WKB and numerical growth rates in a vertically periodic Couette flow with the parameters of Fig. 1 except for a nonzero viscosity like that of gallium: $\nu=3.1\times10^{-3}$. The mode number $n\equiv k_z h/\pi$.

n	WKB γ (s^{-1})	WKB ω_r (s^{-1})	Global γ (s^{-1})	Global ω_r (s^{-1})
1	0.1612	0.9443	0.0965	1.4004
2	0.3911	1.9182	0.3465	2.5164
3	0.5878	2.7084	0.6031	3.2638
4	0.7387	3.2646	0.7907	3.7094
5	0.8356	3.6221	0.8960	3.9549
6	0.8805	3.8366	0.9339	4.0799
7	0.8829	3.9565	0.9241	4.1352
8	0.8543	4.0166	0.8831	4.1512
9	0.8049	4.0400	0.8227	4.1451

$=(0.41,3.90)s^{-1}$, not an accurate result for the growth rate, but considering the width of the gap, the agreement is pleasing.

The growth rates in Table I are of order 1 s^{-1}, as compared to $\sim30\ s^{-1}$ for SMRI in this geometry at the full rotation rate and field planned for the Princeton experiment [21]: $\Omega_1=4000$ rpm, $\Omega_2=533$ rpm, $B_z=5$ kG, and $B_\theta=0$.

C. Finite cylinders: A perturbative approach

In finite nonperiodic cylinders with insulating or partially insulating endcaps, the MHD eigenfunctions are intrinsically two dimensional: they are not separable in r and z. (Separability could be achieved with perfectly conducting endcaps, but then the axial field would be attached to them. This would allow the boundary to exert magnetic forces on the fluid, which seems undesirable and in any case is experimentally less realistic than insulating endcaps.) The purely hydrodynamic problem for $\eta=\infty$ *is* separable, however, if viscosity is neglected so that we may assume no-slip boundary conditions. This suggests a perturbative expansion of the eigenvalue problem in η^{-1}—more properly, $(\mathrm{Re}_m,S)\rightarrow(\epsilon\,\mathrm{Re}_m,\epsilon S)$, with ϵ a small parameter. The cylinders themselves are assumed infinitely long and perfectly conducting; although this is not realistic, it does not result in any attachment of the field to the boundaries, and it allows the magnetic field more easily to be matched onto vacuum solutions that decay as $|z|\rightarrow\infty$ in the regions above and below the fluid. The underlined terms in Eq. (2)–(5) will be neglected because they contribute to the eigenfrequency only at $O(\eta^{-2})$ and higher orders.

We begin with the zeroth-order problem, i.e., for $\eta=\infty$. As noted above, the hydrodynamic boundary conditions

$$\phi=0 \text{ on } r=r_1,r_2 \text{ and on } z=0,h, \tag{13}$$

and inertial-mode equation (7) are separable, so we look for an eigenmode of the form

$$\phi(t,r,z)=e^{-i\omega t}\varphi(r)\sin kz, \quad k=n\frac{\pi}{h}\equiv k_n. \tag{14}$$

The radial function $\varphi(r)$ satisfies

$$\frac{d^2\varphi}{dr^2}+\frac{1}{r}\frac{d\varphi}{dr}+\left[k^2\left(\frac{4a^2}{\omega^2}-1\right)+\frac{1}{r^2}\left(\frac{4abk^2}{\omega^2}-1\right)\right]\varphi=0, \tag{15}$$

assuming a Couette profile $\Omega(r)=a+br^{-2}$ so that $\kappa^2=4a\Omega$, which is satisfied by the Bessel functions $J_\nu(pr)$ and $Y_\nu(pr)$ if

$$\nu^2\equiv 1-\frac{4abk^2}{\omega^2}, \quad p^2\equiv k^2\left(\frac{4a^2}{\omega^2}-1\right). \tag{16}$$

We may thus solve this problem exactly. However, for qualitative information, we notice that if we multiply Eq. (15) by r it becomes

$$\frac{d}{dr}\left(r\frac{d\varphi}{dr}\right)+\left[\frac{1}{\omega^2}\left(4a^2k^2r+\frac{4abk^2}{r}\right)-\left(\frac{1}{r}+k^2r\right)\right]\varphi=0.$$

This is the same form as the Sturm-Liouville problem

$$\frac{d}{dr}\left(P(r)\frac{d\varphi}{dr}\right)+[\lambda R(r)-Q(r)]\varphi=0,$$

$$\varphi(r_1)=0, \quad \varphi(r_2)=0,$$

where

$$P(r)=r,$$

$$R(r)=4a^2k^2r+\frac{4abk^2}{r}>0,$$

$$Q(r)=k^2r+\frac{1}{r}>0,$$

$$\lambda=1/\omega^2.$$

Therefore λ is real and positive [[23], Chap. X]; consequently the frequencies ω which we seek are all real. Furthermore, $\lambda R-Q$ must be positive somewhere within the flow, whence $\omega^2<\max[4a\Omega(r)/(1+k^{-2}r^{-2})]$. There are no modes which grow in time. Thus we conclude that, *all inviscid axisymmetric modes are neutrally stable in the limit of infinite resistivity*. The coefficient $R(r)=\Phi(r)$, the Rayleigh discriminant, so this result is to be expected.

We may arrange for $\phi(r_1)=0$ by taking

$$\varphi_{mn}(r)\equiv J_\nu(pr_1)Y_\nu(pr)-Y_\nu(pr_1)J_\nu(pr). \tag{17}$$

Since we also require $\phi(r_2)=0$, the determinant

$$\Delta(\omega,k)\equiv J_\nu(pr_1)Y_\nu(pr_2)-J_\nu(pr_2)Y_\nu(pr_1) \tag{18}$$

must vanish. The condition $\Delta=0$ defines a discrete set of eigenfrequencies $\omega_{1,n}>\omega_{2,n}>\cdots>\omega_{mn}\cdots>0$ for each $k=k_n$. Let $\phi_{m,n}$ be the complete eigenfunction (14) corresponding to a given k_n and $\omega_{m,n}$. We define an inner product

[here ϕ_{mn} is defined by Eq. (14) with $\varphi(r) \to \varphi_{mn}(r)$]

$$\langle \phi_{m'n'}, \phi_{mn} \rangle \equiv \int_0^h dz \int_{r_1}^{r_2} r dr \bar{\phi}_{m'n'} \phi_{mn}, \tag{19}$$

where the overbar denotes complex conjugation. The eigenfunctions are orthogonal in the sense that $\langle \phi_{mn}, \kappa^2 \phi_{m'n'} \rangle = 0$ if $\omega_{mn}^2 \neq \omega_{m'n'}^2$.

To get the $O(\eta^{-1})$ corrections to ω_{mn}, we must express the magnetic perturbations ψ and b_θ appearing on the right-hand of Eq. (6) in terms of the zeroth-order eigenfunctions ϕ_{mn}. Neglecting the time derivative in Eq. (2) yields

$$D\psi = -\eta^{-1} B_z \partial_z \phi_{mn}. \tag{20}$$

To get b_θ from Eq. (3), we first use Eq. (5) to write $v_\theta \approx (2a/i\omega_{mn}) \partial_z \phi_{mn}$, so that

$$b_\theta \approx -2\eta^{-1} D_T^{-1} \left(\frac{B_\theta}{r} \partial_z \phi_{mn} + \frac{iaB_z k_n^2}{\omega_{mn}} \phi_{mn} \right). \tag{21}$$

. Note that we have replaced ∂_z^2 with $-k_n^2$; we may similarly replace any even power of ∂_z but not an odd power, which changes a $\sin k_n z$ to a multiple of $\cos k_n z$. The operator D_T^{-1} is the inverse of D with the boundary conditions appropriate to b_θ, which are different from those of ϕ [Eq. (13)]:

$$\partial_r^\dagger b_\theta = 0 \text{ at } r = r_1, r_2 \text{ and } b_\theta = 0 \text{ at } z = 0, h. \tag{22}$$

Using Eqs. (20) and (21) to eliminate $D\psi$ and b_θ from Eq. (6) results in

$$(\partial_t^2 D + \kappa^2 \partial_z^2)\phi = -i\omega_{mn}\eta^{-1} \left[(k_n B_z)^2 + 4\left(\frac{-iB_\theta}{r} \partial_z + \frac{\Omega B_z k_n^2}{\omega_{mn}} \right) \times (-D_T^{-1}) \left(\frac{-iB_\theta}{r} \partial_z + \frac{aB_z k_n^2}{\omega_{mn}} \right) \right] \phi_{mn}. \tag{23}$$

On the right-hand side of Eq. (23), the eigenmode and eigenfrequency have been evaluated to zeroth order in η^{-1}. On the left-hand side, we must consider that $\omega \to \omega_{mn} + \delta\omega$ and $\phi \to \phi_{mn} + \delta\phi$, where $\delta\omega$ and $\delta\phi$ are of first order in η^{-1}. We may obtain an expression for $\delta\omega$ by taking the inner product of Eq. (23) with ϕ_{mn} and replacing $i\partial_t \to \omega_{mn} + \delta\omega$ on the left-hand side. The single term involving $\delta\phi$ at $O(\eta^{-1})$ is $\langle \phi_{mn}, (\kappa^2 - \omega_{mn}^2 D)\delta\phi \rangle$, and this vanishes upon integration by parts. On the right side, it is convenient to define the self-adjoint operator

$$H \equiv 2\left(-\frac{B_\theta}{r} i\partial_z + \frac{aB_z k_n^2}{\omega_{mn}} \right) = H^\dagger. \tag{24}$$

At last, then,

$$-\langle \phi_{mn}, D\phi_{mn} \rangle \delta\omega = -\frac{i}{2\eta} \left[(k_n B_z)^2 \langle \phi_{mn}, \phi_{mn} \rangle - \langle H\phi_{mn}, D_T^{-1} H \phi_{mn} \rangle - \frac{2bB_z k_n^2}{\omega_{mn}} \langle \phi_{mn}, r^{-2} D_T^{-1} H \phi_{mn} \rangle \right]. \tag{25}$$

Now D and D_T^{-1} are negative-definite operators. Therefore the only term that can make a positive contribution to the growth rate $\mathrm{Im}(\delta\omega)$ is the last term on the right-hand side, and specifically the part of H involving $B_\theta \partial_z$ since $ab > 0$.

To evaluate $\delta\omega$ from Eq. (25), we need explicit expressions for D and D_T^{-1}. The first is easy enough: it follows from Eq. (7) that $D\phi_{mn} = -[k_n^2 \kappa^2(r)/\omega_{mn}^2]\phi_{mn}$. For D_T^{-1}, we construct the eigenfunctions of D with the boundary conditions (22):

$$D\chi_{jn}(r,z) = -(q_j^2 + k_n^2)\chi_{jn}(r,z), \tag{26}$$

$$\chi_{jn}(r,z) \equiv R_{jn}(r) \sin k_n z, \quad k_n = n\frac{\pi}{h}, \tag{27}$$

where

$$R_{jn} = \begin{cases} J_0(q_j r_1) Y_1(q_j r) - Y_0(q_j r_1) J_1(q_j r) & \text{if } q_j \neq 0; \\ r^{-1} & \text{if } q_0 = 0; \end{cases} \tag{28}$$

and q_j satisfies $J_0(q_j r_1) Y_0(q_j r_2) - Y_0(q_j r_1) J_0(q_j r_2) \equiv 0$. (29)

When applied to χ_{jn}, $D_T^{-1} \to (q_j^2 + k_n^2)^{-1}$. An arbitrary function $f(r,z)$ can be expanded in these eigenfunctions, so that

$$D_T^{-1} f(r,z) = -\sum_n \sum_j (q_j^2 + k_n^2)^{-1} \frac{\langle \chi_{jn}, f \rangle}{\langle \chi_{jn}, \chi_{jn} \rangle} \chi_{jn}(r,z). \tag{30}$$

The important point is that D_T^{-1} turns a function proportional to $\sin k_n z$ into another such function. Therefore $\langle \phi_{mn}, D_T^{-1} \partial_z \phi_{mn} \rangle = 0$, and so the part of H involving $r^{-1} B_\theta i \partial_z$ does not contribute to the expression (25) for the first-order eigenfrequency. This, however, was the only term that might have made for a positive growth rate. We conclude that *at* $O(\eta^{-1})$, *HMRI does not grow in finite cylinders with insulating endcaps*.

The same perturbative method could have been used for periodic vertical boundary conditions; ϕ_{mn} and χ_{jn} would have involved $\exp(ik_z z)$ instead of $\sin k_n z$. The term involving $r^{-1} B_\theta i \partial_z$ in Eq. (25) would then have contributed to the growth rate with the same sign as $-(k_z/\omega_{mn})\Omega B_\theta B_z$. Evaluating this term, we conclude that in highly resistive periodic flows, (i) unstable modes propagate axially in the direction of the background Poynting flux—as found in WKB; and (ii) the instability occurs only if $\beta > ak_z r/\omega_{mn}$ somewhere within the gap. Given the upper bound on ω_{mn}^2 noted above, it follows that $\beta^2 > \min[4a/\Omega(r)]$.

We have written MATLAB procedures to evaluate Eq. (25). The results confirm our conclusions above. When periodic boundary conditions are used, the perturbative result matches the growth rate found from our radially global linear code to three digits in sufficiently resistive cases: e.g., $\gamma = 1.89 \times 10^{-3} \Omega_1$ in the Princeton geometry with $\mathrm{Re_m} = 0.1$,

$S=0.043$, $\Omega_2/\Omega_1=0.1325$, and $\beta=2$. But when insulating endcaps are imposed, the perturbative estimate of the growth rate is always negative.

D. Finite cylinders: Two other approaches

Here we analyze finite cylinders by approximations that do not require large resistivity: by a variant of WKB and by direct axisymmetric numerical simulations.

In the modified WKB approach, perturbations are again assumed to vary as $\exp(ik_r+st)$ with a common complex growth rate $s\equiv -i\omega$ and radial wave number $k_r=\pi/(r_2-r_1)$, but the vertical dependence is treated differently. With the t and r dependence factored out, the linearized equations of motion reduce to homogeneous ordinary differential equations with coefficients independent of z. Elementary solutions of these equations exist with exponential dependence on z; however, since the vertical boundaries are not translationally invariant, the wave number k_z need not be real, and growing modes can be linear combinations of the elementary exponential solutions with the same ω but different k_z. The vertical magnetic boundary conditions require the fields to match onto a vacuum solution that decays exponentially as $|z|\to\infty$ in the space $r_1\leqslant r\leqslant r_2$ between the extended conducting cylinders:

$$z=0: \quad \phi=b_\theta=0, \quad \partial_z\psi=|k_r|\psi;$$

$$z=h: \quad \phi=b_\theta=0, \quad \partial_z\psi=-|k_r|\psi. \tag{31}$$

We search iteratively for such modes as follows. Given a trial value for s, the dispersion relation (9) has six roots—in general complex—for the vertical wave number, which can be regarded as algebraic functions of the growth rate: $\{k_{z,\alpha}(s)\}$, $\alpha\in\{1,\ldots,6\}$. We seek a mode in the finite cylinder of the form

$$\boldsymbol{q}(t,r,z)\equiv[\phi,v_\theta,\psi,b_\theta]^T=e^{st+ik_r r}\sum_{\alpha=1}^{6}Y_\alpha\boldsymbol{q}_\alpha\exp(ik_{z,\alpha}z). \tag{32}$$

Each term in the sum above is the elementary solution corresponding to a particular root $k_{z,\alpha}(s)$, with $\boldsymbol{q}_\alpha$ a four-component column vector; these elementary solutions are superposed with constant weights $\{Y_\alpha\}$. Substitution into the boundary conditions (31) yields a sixth-order homogeneous linear system for the $\{Y_\alpha\}$. Nontrivial solutions exist only if the determinant $\mathcal{D}(s)$ of this system vanishes. The equation $\mathcal{D}(s)=0$ is transcendental and we cannot solve it analytically, but a numerical nonlinear zero-finding algorithm recovers the roots for s.

We have checked this procedure by replacing Eq. (31) with periodic boundary conditions and comparing the results with direct solutions of the dispersion relation (9). Also, we find reasonably good agreement with growth rates determined from ZEUS2D simulations of a narrow-gap configuration with insulating boundaries (see below). However, for sufficiently large resistivity, no roots with positive $\mathrm{Re}(s)$ are found, in agreement with the perturbative results of Sec. II C.

For the ZEUS2D simulations, we represent the poloidal magnetic field at $z\leqslant 0$ and $z\geqslant h$ by flux functions $\Phi_\pm(r,z)$ satisfying $b_r\boldsymbol{e}_r+b_z\boldsymbol{e}_z=r^{-1}\boldsymbol{e}_\theta\times\boldsymbol{\nabla}\Phi$ and $\boldsymbol{\nabla}\times\boldsymbol{b}=0$. The latter implies $r\partial_r(r^{-1}\partial_r\Phi)+\partial_z^2\Phi=0$, which is solvable by separation of variables since we require $\Phi=0$ on the vertically extended conducting cylinders. The elementary solutions are

$$\Phi_k(r,z)\propto re^{-k|z-z_0|}[Y_1(kr_1)J_1(kr)-J_1(kr_1)Y_1(kr)],$$

for an infinite discrete set of non-negative values of k determined by $\Phi_k(r_2,z)=0$. At each endcap, we match the vertical field b_z protruding from the fluid with a superposition of vacuum solutions of this form, and thereby obtain a boundary condition relating b_z and b_r. Of course $b_\theta=0$ at these boundaries since the current along the axis is constant.

We have performed simulations with insulating endcaps for the parameters of Fig. 1. We find a complex growth rate $s\approx 0.51+4.18i\ \mathrm{s}^{-1}$, as compared to $s\approx 0.37+3.68i\ \mathrm{s}^{-1}$ from the modified WKB approach (31) and (32) above. Considering the approximate nature of the latter approach, the agreement is satisfactory. We have also carried out ZEUS2D simulations with insulating endcaps in the wide-gap experimental geometry $[(r_1,r_2,h)=(7.1,20.3,28)\ \mathrm{cm}]$. Here we find a growth rate $\sim 0.27\ \mathrm{s}^{-1}$, as opposed to $\sim 1.06\ \mathrm{s}^{-1}$ with periodic boundaries. We conclude that insulating endcaps lower the growth rate, even in flows of moderate $(\mathrm{Re}_\mathrm{m},S)$.

A limitation of our direct simulations is that since we use explicit time stepping, we cannot explore very large resistivities [21]. The modified WKB approach does not suffer from any restriction on η, but it is not trustworthy for wide gaps. The concordance between the two approaches where both are applicable—namely for narrow gaps and moderate $(\mathrm{Re}_\mathrm{m},S)$—inclines us to trust results obtained from one of these approaches in regimes where the other is not applicable. In particular, the modified WKB method predicts that highly resistive flows are completely stable in finite cylinders, at least for narrow gaps. The perturbative analysis of Sec. II C reaches the same conclusion for gaps of any width, but that analysis is valid at $O(\eta^{-1})$ only.

III. DISCUSSION AND CONCLUSIONS

We have analyzed the linear development of helical magnetorotational instability in a nonideal magnetohydrodynamic Taylor-Couette flow, paying particular attention to the effects of the axial boundary conditions. A number of complementary approximations and numerical methods have been used.

For infinitely long or periodic cylinders, we confirm that there is an axisymmetric MHD instability that persists to smaller magnetic Reynolds number and Lundquist number in the presence of *both* axial and toroidal background magnetic field than the standard MRI that exists for axial field alone. The mode is an overstability and propagates axially in the direction of the background Poynting flux $-r\Omega B_\theta B_z/\mu_0$. In highly resistive flows, the mode is a weakly destabilized hydrodynamic inertial oscillation. Growth depends also on the ratio of shear to rotation, *i.e.*, Rossby number: for all aspect ratios r_2/r_1 that we have explored, and certainly for narrow

gaps, the Keplerian Rossby number is stable.

We have also considered finite cylinders with insulating endcaps, which are closer to experimental reality but which do not permit traveling modes that propagate indefinitely along the axis. Astrophysical disks also have limited vertical thickness. These boundary conditions reduce the growth rate of the helical mode and stabilize highly resistive flows entirely, at least in the absence of viscosity and viscous boundary-layer effects.

Here some comments are in order regarding a recent paper that claims to have observed HMRI in the Potsdam PROMISE experiment [9]. It is reported that when the axial current lay in the range where HMRI was expected (based on an analysis of infinite cylinders), persistent fluctuations were measured by ultrasonic velocimetry that appeared to form axially traveling waves, consistent with expectations for HMRI.

These claims do not necessarily contradict our analysis. An exponential growth rate has not been reported, which would have been a clear signature of a discrete linear unstable mode. Rather than a global instability, we suspect that the observed fluctuations represent excitation by processes outside our inviscid analysis, followed by transient magnetic amplification as the disturbances propagate along the axis. This is what one might expect, given an appropriate source of excitation, when the local WKB dispersion relation predicts instability but the boundary conditions are not compatible with a global mode. Data given in [9] clearly show vibrations at the rotation frequencies of the cylinders themselves; these or other experimental imperfections might have excited the waves, although the peaks in the temporal power spectrum attributed to the waves appear to be broader than those at the cylinder frequencies and are distinct from them. Further evidence that may bear on the excitation mechanism comes from another recent publication [24], which reports numerical axisymmetric simulations for parameters approximating the experiment but for both axially infinite (actually periodic) and finite cylinders. External vibrations, roughness, and magnetic interaction with the boundary need not exist in the simulations, but since no-slip conditions are applied at the endcaps, which rotate as in the experiment, viscous boundary layers should exist in the finite cylinders. In [24], a clear vertically traveling mode is seen in the infinite cylinders, but in the finite ones, the velocity fluctuations, though sustained, appear to be unsteady and to have a fluctuating spatial pattern. At the Reynolds numbers where these fluctuations were reported, $\mathrm{Re} \geqslant 900$, Ekman circulation in purely hydrodynamic simulations by [25] was also unsteady.

The above speculations aside, the fact remains that the inviscid analyses of the present paper do not apply to situations where viscosity may be important, as they probably are in the PROMISE experiment. Viscous effects must be included to model such experiments reliably. On the other hand, viscous boundary layers lead to an exchange of angular momentum between the fluid and its container. Such exchanges are not expected to be important in astrophysical disks, so it may be appropriate to neglect viscosity when one is interested in astrophysically important modes.

Thus the relevance of HMRI to astrophysical disks is questionable, although it may be relevant to stellar interiors and jets, where the magnetic geometry and the Rossby number may be more favorable. Also, HMRI may have theoretical significance that goes beyond its direct applications. It is not understood why linearly and axisymmetrically stable rotating flows are often also nonlinearly and nonaxisymmetrically unstable, especially since subcritical transition does occur at some Rossby numbers [26]. The fact that even a very poorly coupled magnetic field can sometimes linearly destabilize such flows hints that it might also affect nonlinear transition.

ACKNOWLEDGMENTS

The authors would like to thank James Stone for the advice on the ZEUS code. This work was supported by the U.S. Department of Energy, NASA under Grant Nos. ATP03-0084-0106 and APRA04-0000-0152, the National Science Foundation under Grant Nos. AST-0205903 and PHY-0215581, and in part by the U.S. Department of Energy under Grant No. DE-FG02-05ER25666 (to I.H.).

[1] S. Balbus and J. Hawley, Rev. Mod. Phys. **70**, 1 (1998).
[2] E. P. Velikhov, Sov. Phys. JETP **36**, 1398 (1959).
[3] S. Chandrasekhar, Proc. Natl. Acad. Sci. U.S.A. **46**, 253 (1960).
[4] S. Balbus and J. Hawley, Astrophys. J. **376**, 214 (1991).
[5] J. Hawley, C. Gammie, and S. Balbus, Astrophys. J. **470**, 742 (1995).
[6] A. Brandenburg, A. Nordlund, R. Stein, and U. Torkelson, Astrophys. J. **446**, 741 (1995).
[7] R. Matsumoto and T. Tajima, Astrophys. J. **445**, 767 (1995).
[8] D. R. Sisan, N. Mujica, W. A. Tillotson, Y. M. Huang, W. Dorland, A. B. Hassam, T. M. Antonsen, and D. P. Lathrop, Phys. Rev. Lett. **93**, 114502 (2004).
[9] F. Stefani *et al.*, e-print astro-ph/0606473.
[10] H. Ji, J. Goodman, and A. Kageyama, Mon. Not. R. Astron. Soc. **325**, L1 (2001).
[11] J. Goodman and H. Ji, J. Fluid Mech. **462**, 365 (2002).
[12] K. Noguchi, V. I. Pariev, S. A. Colgate, H. F. Beckley, and J. Nordhaus, Astrophys. J. **575**, 1151 (2002).
[13] R. Hollerbach and G. Rüdiger, Phys. Rev. Lett. **95**, 124501 (2005).
[14] G. Rüdiger, R. Hollerbach, M. Schultz, and D. Shalybkov, Astron. Nachr. **326**, 409 (2005).
[15] I. Herron and F. Soliman, Appl. Math. Lett. **19**, 1113 (2005).
[16] C. F. Gammie, Astrophys. J. **457**, 355 (1996).
[17] M. Ilgner and R. P. Nelson, Astron. Astrophys. **445**, 205 (2006).
[18] E. Knobloch, Mon. Not. R. Astron. Soc. **255**, 25P (1992).
[19] E. Knobloch, Phys. Fluids **8**, 1446 (1996).
[20] I. Herron and J. Goodman, ZAMP **57**, 615 (2006).

[21] W. Liu, J. Goodman, and H. Ji, Astrophys. J. **643**, 306 (2006).
[22] J. Stone and M. Norman, Astrophys. J., Suppl. Ser. **80**, 753 (1992).
[23] E. L. Ince, *Ordinary Differential Equations* (Dover, New York, 1956).
[24] J. Szklarski and G. Rüdiger, Astron. Nachr. **327**, 844 (2006).
[25] A. Kageyama, H. Ji, J. Goodman, F. Chen, and E. Shoshan, J. Phys. Soc. Jpn. **73**, 2424 (2004).
[26] G. Lesur and P.-Y. Longaretti, Astron. Astrophys. **444**, 25 (2005).